Journal of Food Engineering 387 (2025) 112336

Contents lists available at ScienceDirect

Journal of Food Engineering

journal homepage: www.elsevier.com/locate/jfoodeng

Microwave cavity antenna for automatic detection of chicken breast muscles affected by wooden breast defect

Eleonora Iaccheri [a,b], Francesca Soglia [a,b,*], Massimiliano Petracci [a,b], Luigi Ragni [a,b]

[a] Department of Agricultural and Food Sciences, Alma Mater Studiorum, University of Bologna, Cesena, Italy
[b] Interdepartmental Centre for Agri-Food Industrial Research, Alma Mater Studiorum, University of Bologna, Cesena, Italy

ARTICLE INFO

Keywords:
Wooden breast
Microwave antenna
Automatic detection
Poultry industry

ABSTRACT

Over the past years, artificial selection for meat-type (broiler) chickens has resulted in improved production efficiency, but also in an increased incidence of skeletal muscle abnormalities. In particular, wooden breast (WB) abnormality causes abrupt changes in meat quality and enormous economic losses. Thus, the poultry processing industry requires a reliable method to detect the abnormality in production lines in a non-destructive and contactless way. The present research aimed to evaluate the effect of WB on dielectric properties to develop a potential online technique to distinguish unaffected from affected breasts. Sixty-five *pectoralis major* muscles were picked 3 h post-mortem from the same flock (42-day-old broilers, 2.8 kg average live weight) and classified by visual inspection according to their phenotype as normal (N, not showing not any signs of the WB condition; n = 33) or WB (exhibiting extensive hardened areas and stiffness perceived by manual palpation throughout the entire fillet; n = 32). WB muscles exhibited remarkably higher values of dielectric constant and loss factor in a wide range of the explored frequencies (200 MHz–14 GHz), suggesting higher water mobility and a higher solvate capacity; this makes the electromagnetic technique for classification promising. Based on the above evidence, a rapid microwave electric technique in the range 1.5 GHz–3 GHz was developed for the online detection of WB. Indeed, combining the use of a cavity antenna (vector network analyzer instrumental chain with partial least square – discriminant analysis), this technique correctly classified 100% of the validation test set.

1. Introduction

Artificial selection over the past 60 years has led to rapid growth rates and increased meat yield in broilers (meat-type chickens), but it also introduced some challenges such as an increased occurrence of growth-related breast muscle abnormalities (i.e., white striping, wooden breast and spaghetti meat) (Barbut et al., 2024; Soglia et al., 2021). Literature reports have depicted that defects in *Pectoralis major* muscle result in qualitative and economical devaluation of broiler breast meat (Mudalal et al., 2015; Pang et al., 2020a,b; Petracci et al., 2019; Soglia et al., 2016, 2021; Wang et al., 2023). Downgrading and quality losses caused by growth-related abnormalities have caused huge economic losses for the poultry industry estimated in North America for over 1 billion USD per year (Barbut et al., 2024; Wang et al., 2023). Considering the increasing world demand for poultry products, growth-related muscle abnormalities are expected to raise.

Wooden breast (WB) is one of the muscle abnormalities that affects meat quality. This defect is characterized by hardened texture and pale areas along with petechial hemorrhages mainly in the cranial or caudal portion of the breast muscle (Petracci et al., 2019).

Accordingly, the poultry industry requires a reliable method to detect this abnormality in production lines in a non-destructive and contactless way. One of the biggest advantages of having automatic and objective real-time information is the reduced cost of manual inspection, associated with increased work efficiency and minimization of waste, thereby augmenting the sustainability of the production process (Barbut et al., 2024). Although the distinctive characteristics of WB can be described in terms of physical properties (e.g. hardness, rigidity, change in visual appearance), its detection is difficult because of the random distribution of the occurrence and different severities of the defects' intensity (Morey et al., 2020).

Recently, some applications of online methods able to detect WB in manufacturing lines have been reported, including near-infrared spectroscopy (Geronimo et al., 2019; Wold et al., 2017), and bioelectrical impedance analysis was used as a tool to differentiate between normal and severe WB meat, even if the samples had to be in contact with probe

* Corresponding author. Department of Agricultural and Food Sciences, Alma Mater Studiorum, University of Bologna, Cesena, Italy.
E-mail address: francesca.soglia@unibo.it (F. Soglia).

https://doi.org/10.1016/j.jfoodeng.2024.112336
Received 18 July 2024; Received in revised form 9 September 2024; Accepted 23 September 2024
Available online 26 September 2024

(Morey et al., 2020). Optical coherence tomography (OCT) was applied to classify chicken breast fillet according to WB severity (Ekramirad et al., 2024) and image analysis was applied to detect WB in broiler carcasses (Caldas-Cueva et al., 2021) and breast fillets (Yoon et al., 2022). In addition, a spectrophotometric system able to detect white striping abnormality in whole chicken carcass has also been investigated (Traffano-Schiffo et al., 2017). Despite some already existing applications, inexpensive technologies that are capable of measuring WB on breast fillets in the manufacturing line based on the electromagnetic wave interaction are still required.

Dielectric properties could represent an opportunity to develop a spectrometer that is able to investigate the bio-physical properties of chicken breast in a non-destructive, inexpensive, and contactless way. Dielectric properties describe the behavior of a material under an electromagnetic field. Permittivity is the physical quantity describing the dielectric properties as a function of the absorption, dissipation, and reflection of electromagnetic energy. The permittivity is mathematically described as a complex number composed of the dielectric constant (related to energy absorption and storage) and loss factor (mainly linked to energy dissipation) of the real and imaginary part, respectively (Asami, 2002; Nelson, 2010). Dielectric properties have been successfully applied to investigate a wide range of biological products (Iaccheri et al., 2023a,b; Kent and Anderson, 1996; Liu et al., 2012; McKeown et al., 2012; Nelson, 2010; Nunes et al., 2006; Ragni et al., 2007) and particularly poultry meat (Tran and Stuchly, 1987; Nelson et al., 2007; Tanaka et al., 2000; Traffano-Schiffo et al., 2021).

The objective of the present research was to study the dielectric properties of chicken breasts affected by WB. Based on the results obtained, an inexpensive and reliable method that exploits the interaction of electromagnetic waves, in the microwave range (1.5–3.0 GHz), was developed to detect the WB defect.

2. Materials and methods

2. collection

A total of 65 chicken breasts were selected at 3 h post-mortem in a commercial slaughter plant on different sampling days. The chicken breasts, belonging to the same flock of animals with homogeneous characteristics, were selected and classified as unaffected N (n = 33) and affected by WB (n = 32) (Fig. 1). In detail, samples were classified according to their visual appearance (macroscopically normal or showing pale and hardened areas along with petechial haemorrhages). To avoid misleading results, only severe WB cases were considered. The samples were kept at 5 ± 1°C.

2.2. Dielectric properties

Dielectric properties were assessed at 5°C in triplicate, by moving the probe in three different position of the breast, in a wide radiofrequency range of 200 MHz to 14 GHz using an open-ended coaxial probe instrumental chain. The acquisitions were carried out by means of an open-ended coaxial probe (DAKS-3.5 probe, Zurich, Switzerland) connected to a vector network analyzer (Copper Mountain, Indianapolis USA) and interfaced via USB with a PC (Fig. 2).

The DAK Software (Installer 2.6.1.7) was used for acquisition and calibration procedures. Calibration was carried out using a custom calibration kit (Speag DAK-3.5/1.2 circuit block, metal strip set, and 0.6 l of DAK SL AAH U16 BD verification liquid), accounting for open, short and load determinations.

The chicken breasts were positioned on plastic support and brought into contact with the probe with an elevated platform to avoid probe and cable movements, which is a possible source of signal noise.

The dielectric constant (ε′), and the loss factor (ε’’) of the chicken breast belonging from the two classes, N and WB, were directly obtained by the DAK software. Each spectrum is composed by 920 data points

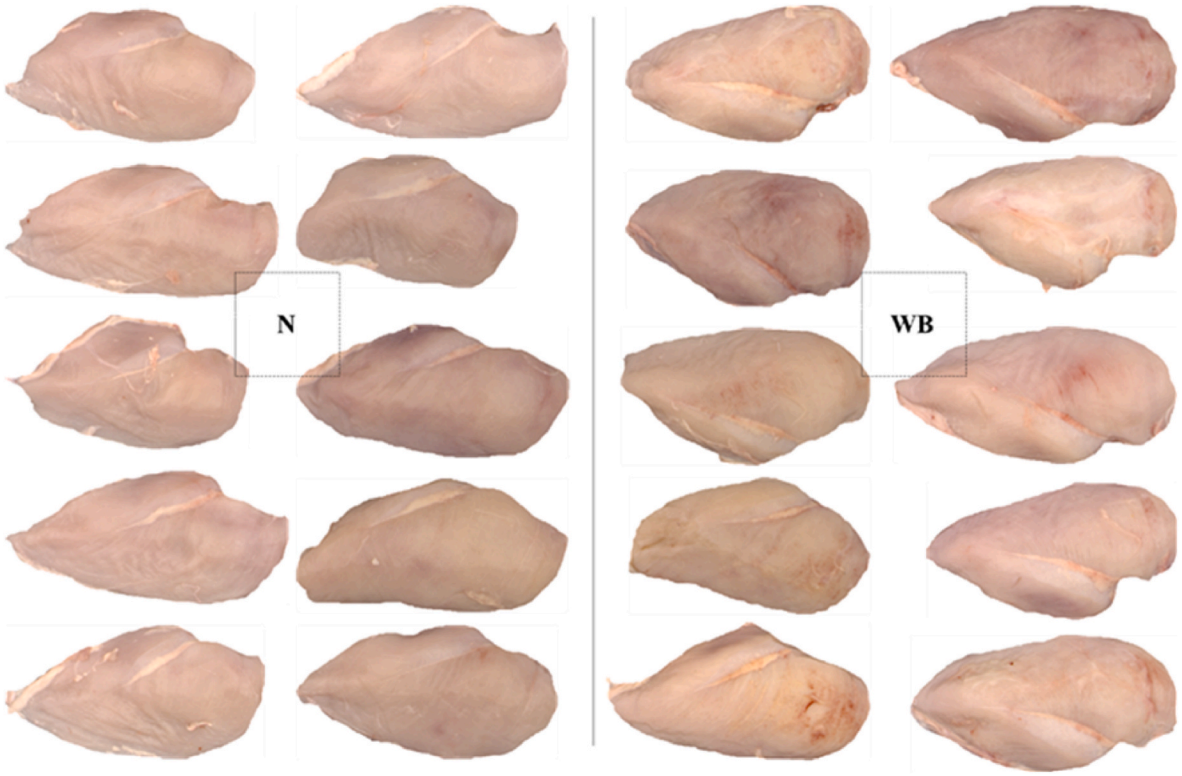

Fig. 1. Chicken breasts classified as unaffected (N) and affected by wooden breast (WB) (photos were captured with a visual analyzer VA400 IRIS Alpha M.O. S., France).

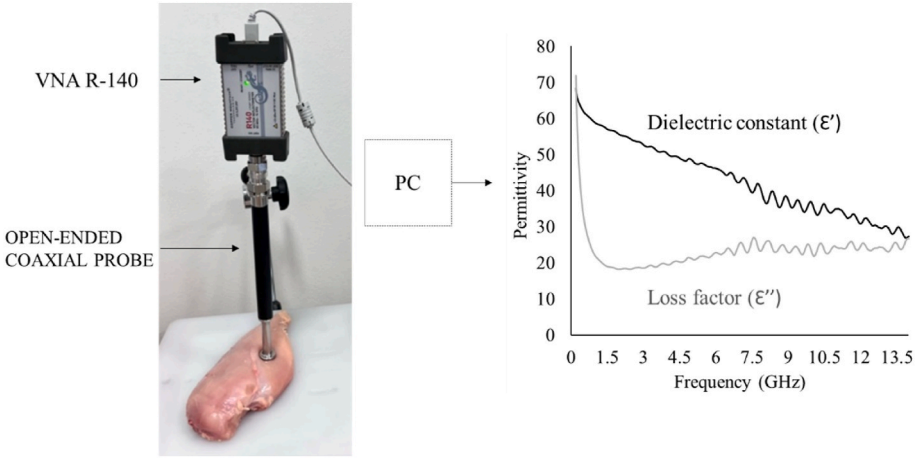

Fig. 2. Open-ended coaxial probe instrumental chain for assessment of dielectric properties.

subsequently used for statistical elaboration.

2.3. Instrumental chain with cavity antenna

With the intention of developing an affordable technique to identify WB, a contactless and rapid instrumental chain was set up based on transmission line theory. When a transmission line is terminated with an unmatched load (different dielectric characteristics), two waves are present, the incident and the reflected ones. In particular, a radio-frequency incident signal is acquired on one port and part of this signal is loss in absorption or dissipation, while part is reflected and sent back to the probe. These two components overlap and the resulting one is defined as a standing wave. Dielectric mismatch is measured by the scattering parameters of the reflected wave (real and imaginary parts of S11). The real and imaginary parts of S11 are related to impedance by the reflection coefficient (Γ):

$$\Gamma = \frac{Z_l - Z_0}{Z_l + Z_0} \text{ and } |\Gamma| = \sqrt{(S11_{re}^2 + S11_{im}^2)}$$

where Z_l is the load impedance, Z_0 is the line characteristic impedance, and $S11_{re}$ and $S11_{im}$ are the real (resistive) and imaginary part (reactive) of S11.

The ratio between the maximum (Vmax) and minimum (V min) standing wave amplitude is known as the standing wave ratio (VSWR).

$$VSWR = \frac{1 + |\Gamma|}{1 - |\Gamma|}$$

The real and imaginary parts of the S11 and the SWR spectra were acquired with an instrumental chain composed by a rectangular cavity antenna (dimensions: width 96 × height 46 × length 118 mm) connected to a VNA (Vector Network Analyzer; Copper Mountain, Indianapolis, USA) (Fig. 3).

Calibration of the VNA was performed using the producer's calibration kit (N1801, Copper Mountain USA), accounting for open, short and load calibration. The acquisitions were conducted in triplicate, at 5°C, in the frequency range from 1.5 GHz to 14 GHz. The resonant frequencies (the frequencies at which the reactance is zero) of the antenna were 1.56 and 2.46 GHz (in air). The breasts were not placed in contact with the antenna in order to carry out contactless measurements. The real and imaginary parts of the S11 and the SWR were automatically collected by the own VNA software.

2.4. Statistical analysis

Dielectric spectra belonging to the open-ended coaxial probe chain were only used to characterize the material. No processing was done. The raw spectral signals obtained with the cavity antenna were composed of 301 points. Firstly, Principal Component Analysis (PCA)

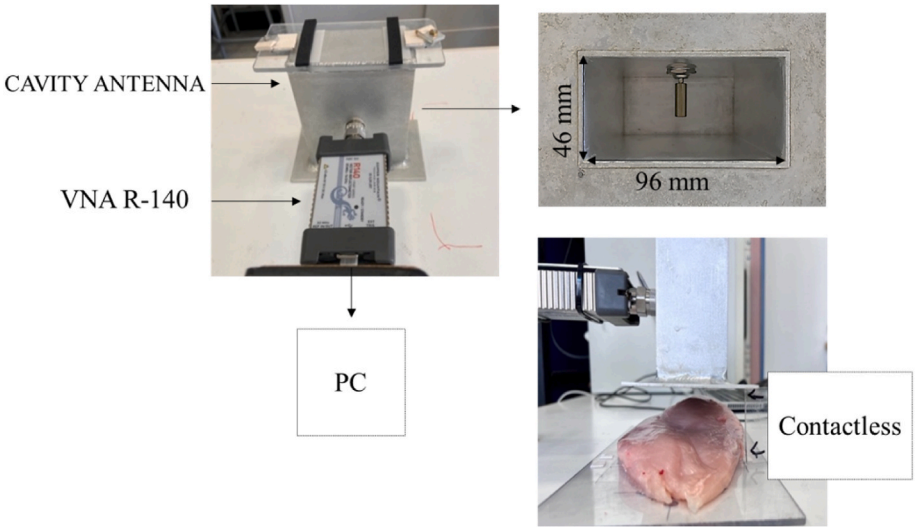

Fig. 3. Instrumental chain set up, with cavity antenna and vector network analyzer. On the upper right, the internal section dimensions of the probe are reported.

was implemented to explore the variability in multivariate data sets and understand possible relationships between samples (N and WB) and the variables (X, spectral data). By reducing the variable numbers in the principal components (PCs), the entire variability of the dataset can be studied. PCA was also useful for the outlier selection made through the score plot (6 samples were removed, all WB). Spectral range selection was made by a loading weights plot, considering that the highest values (in absolute) have a large contribution in explaining the variability of the two groups in the related frequencies. PCA was also used to select the external dataset for the subsequent classification model validation. Samples were selected from the left, the right, and the central PCA score plot to build an external-validation set with the maximum sample variability.

PLS-DA was chosen as a rapid screening method to classify samples, with the possibility of directly implementing the algorithm. PLS-DA was performed to classify samples into two groups unaffected (N) and affected by WB. PLS-DA is a supervised method in which the class attribution is already defined as 1 (class N) and −1 (class WB). The PLS-DA determines whether a sample belongs to class 1 or class −1. The closer is the sample to those values, the more similar the class. The class's dividing line is 0. Twelve samples were selected from PCA, which were not included in the training stage, and used to validate the models, performing an external validation. External validation is very helpful to understand how the model will perform considering new future samples.

In addition, performance of the PLS-DA model was evaluated as a function of the coefficient of determination (R^2) of calibration and validation and related root mean square error of prediction (RMSEP), the standard error of prediction (SEP), the systematic error BIAS, and the residual prediction deviation (RPD). Bias is a measure of the accuracy of the prediction model and SEP is the expression of the precision of the results, corrected for Bias. The RPD is the ratio between the standard deviation of the reference values and the SEP. RPD is an index of practical utility to understand the goodness of model estimation. Values of RPD higher than 2 are considered suitable for analytical data (Wold et al., 2001).

Multivariate data analysis was performed with The Unscrambler software (Unscrambler software, version 9.7, CAMO, Oslo, Norway).

3. Results and discussion

The dielectric constant and loss factor of all chicken breasts that were unaffected (N) and affected by WB at 5°C are shown in Fig. 4.

The dielectric constant of both N and WB chicken breasts decreased as a function of frequency due to the dispersion events, typical of the biological materials and mainly attributable to water/solid dynamics (Trabelsi, 2015). The dielectric loss factor, more dominated by ionic conductivity in the lower portion of the frequency range explored, did not show spectral changes, while at higher frequencies these are revealed and mainly attributable to the dipolar rotation of the water molecules. Similar results in terms of dielectric constant and loss factor have been previously reported (Nelson, 2010; Trabelsi, 2015). It is widely known that dielectric properties respond to water content, but also to water mobility (Iaccheri et al., 2023a,b; Iaccheri et al., 2015; Nelson, 2010; Trabelsi, 2015). Thus, further considerations can be drawn by observing the different behavior of N and WB samples. The WB condition is previously reported to cause alteration of water content and reduction of water holding capacity in broiler breast fillet (Choi et al., 2024; Sun et al., 2022). WB affects the proportion of extra-myofibrillar, by increasing its content, and results in a lower intra-myofibrillar and hydration water (Pang et al., 2020a,b; Zhang et al., 2022) thus influencing its physical behavior, such as mechanical (Choi et al., 2024; Tasoniero et al., 2017), rheological, and gelling properties (Zhang et al., 2020). Previous investigations suggested the importance of water solid relation characterizing WB samples, all confirming a higher water mobility in raw WB samples (Choi et al., 2024; Pang et al., 2020a,b; Soglia et al., 2021; Tasoniero et al., 2017; Zhang et al., 2022, 2020), as well as in marinated breast meat (Zhang et al., 2022). Accordingly, the dielectric properties presented herein show higher values of dielectric constant and loss factor for WB samples, which are typical of products with higher water content and water mobility.

Consequently, the dielectric properties changes represent an opportunity to set up an automatic sensor able to identify chicken breasts that are affected and unaffected by WB abnormality.

Regarding the results obtained for cavity antenna, all raw spectral data of real and imaginary parts of S11 and VSWR for N and WB samples at 5°C are shown in Fig. 5.

The frequency dependence scattering parameters and VSWR measured at 5°C showed a spectral variation in terms of peak intensity and slope, as a function of WB abnormality, confirming the results of dielectric properties. In particular, it is possible to observe that the low-frequency range is characterized by large spectral variability.

Chicken breasts are deboned and processed in plants with possible temperature fluctuation. Thus, to verify the extent of signal variation as a function of temperature, a test was carried out. One chicken breast for each experimental group was placed at room temperature (22°C) to measure the dielectric properties during a slow increase in temperature, from 6°C to 16°C, considering that a thermal condition should be avoided. Fig. 6 shows a typical variation of the VSWR parameter in frequency at the selected temperatures for unaffected (N) and affected (WB) breasts.

The VSWR for N and WB samples showed only a slight variation in the temperature range investigated. The variation of the spectral response as a function of temperature was considerably lower than the sample variation induced by WB abnormality and thus should not compromise the technique's applicability in poultry processing lines.

S11 parameters were then employed to perform a PCA in the whole

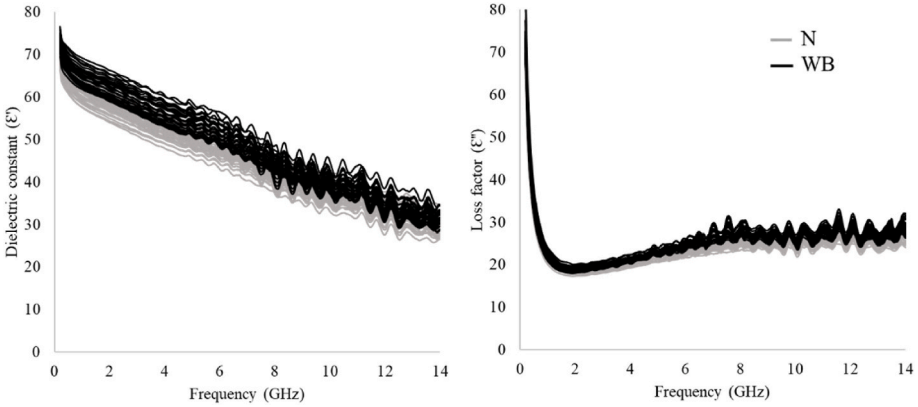

Fig. 4. Dielectric constant and loss factor in the frequency range 200 MHz-14GHz.

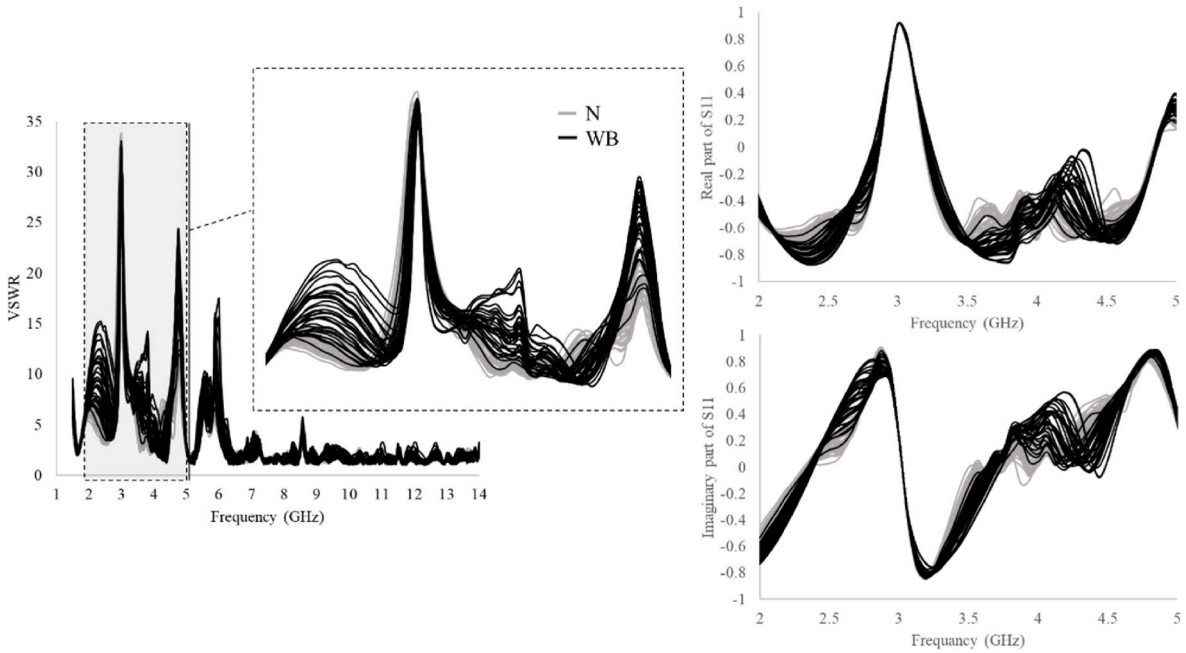

Fig. 5. VSWR, the real and imaginary part of S11 spectra for N and WB samples.

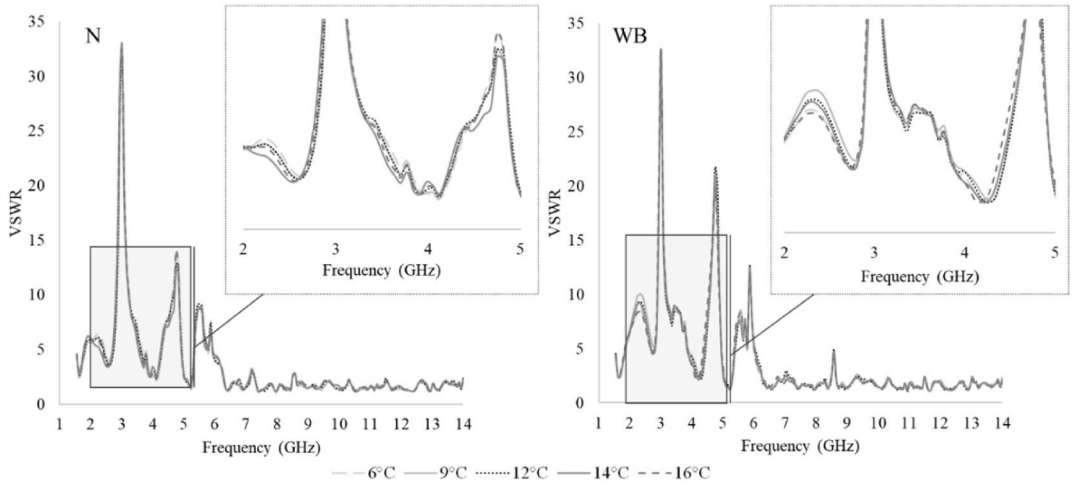

Fig. 6. Temperature influences of the VSWR for N and WB samples.

spectral range, the loading weights plot are shown (Fig. 7).

The loadings weight of the first two PC allow to select a reduced spectral range in which variables give the most important contribution to explain data variability. The real, imaginary part and VSWR highest frequency range are characterized by lower loadings weight. As Fig. 7 shown, the huge difference is revealed for VSWR parameter. It should be considered that increasing the frequency range, increase also the noise. Therefore, data were then selected in the frequency range from 1.5 to 9 GHz.

Accordingly, the PCA of the real, the imaginary part, and the SWR was then repeated in the selected frequency range and shown in Fig. 8.

In Fig. 8, all the PCA have a very good separation according to the presence or absence of WB abnormality, especially along PC1. The highest value of explained variance was achieved with the VSWR parameter with 87% considering PC1 and 9% concerning PC2. It should be noted that WB abnormality can affect a variable superficial area of the sample and with different degrees of intensity. Thus,a low incidence of the defect causes only small changes in the electrical signal and a slight superimposition in the PCA is therefore expected.

As previously mentioned, the PCA was used as a screening method to subsequently classify with the PLS-DA, allowing validation of the model which is useful to understand how the it will work with future samples. The results of PLS_DA in the selected frequency range (1.5–9.0 GHz) are reported in Fig. 9.

As can be seen in Fig. 9, PLS-DA correctly classified 100% of the samples into unaffected (N) and affected (WB) breasts for all the scattering parameters considered.

The validation dataset was used during the calibration process to obtain a more reliable error, thereby avoiding model underfitting and overfitting. All the parameters considered in the validation stage of the regression are reported in Table 1.

The external data set of the PLS-DA models used for the S11 real, S11 imaginary parts and VSWR concerned 12 elements each. Very good coefficients of determinations were obtained for all the scattering parameters, even if the best result was obtained by the real part of S11 with R^2 of 0.935. According to bias, which is near zero, the model does not

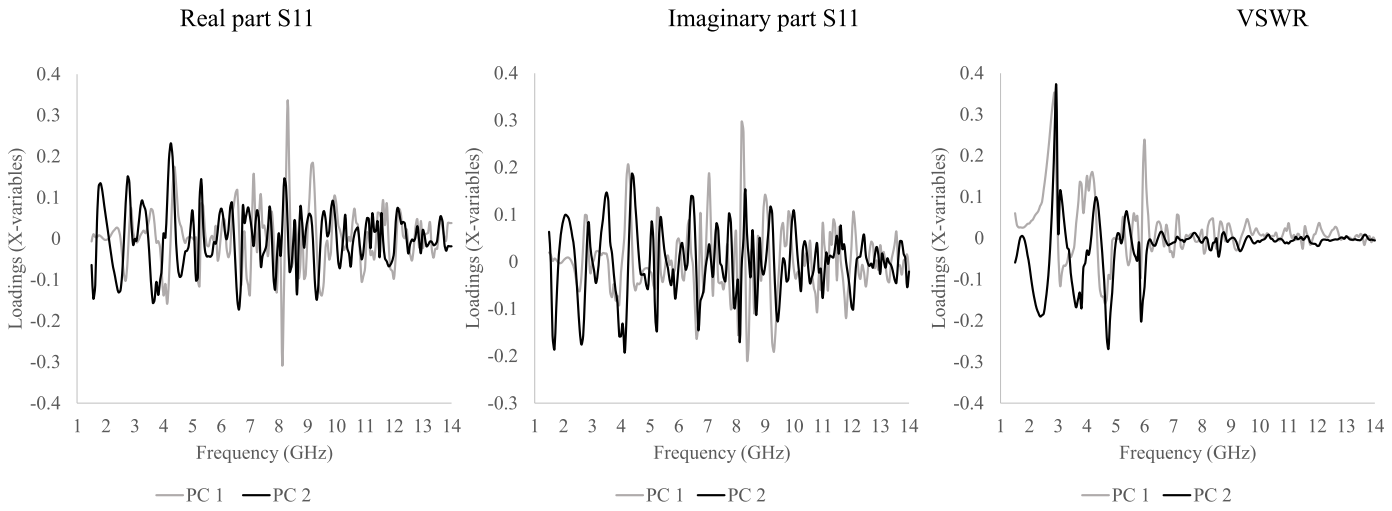

Fig. 7. Loadings weight of the first two Principal Component considering real, imaginary part and VSWR parameters.

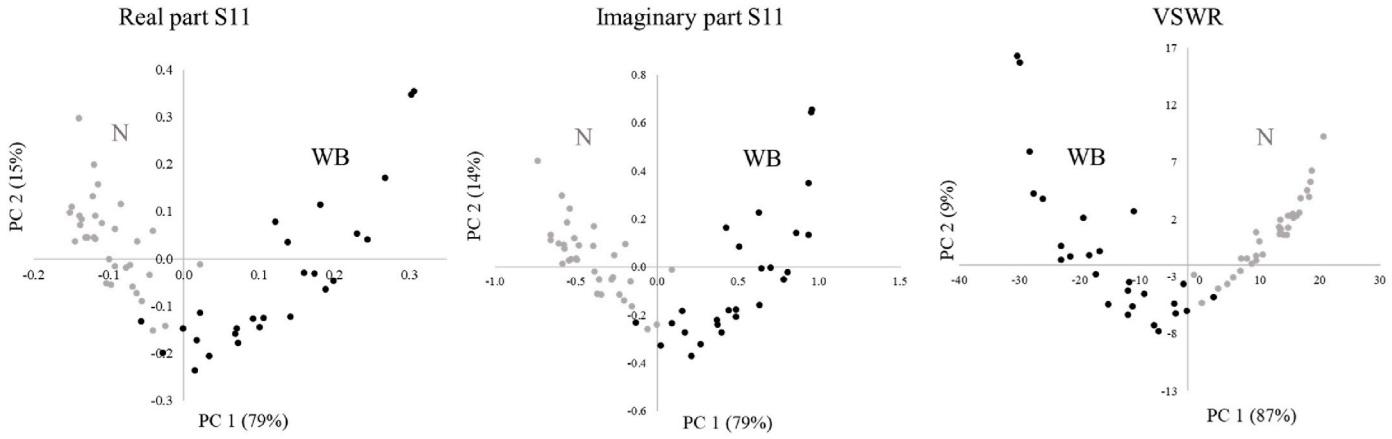

Fig. 8. PCA of the real, imaginary part, and VSWR grouping N and WB samples. Principal component (PC) 1 and 2 and related percentages to explain variance.

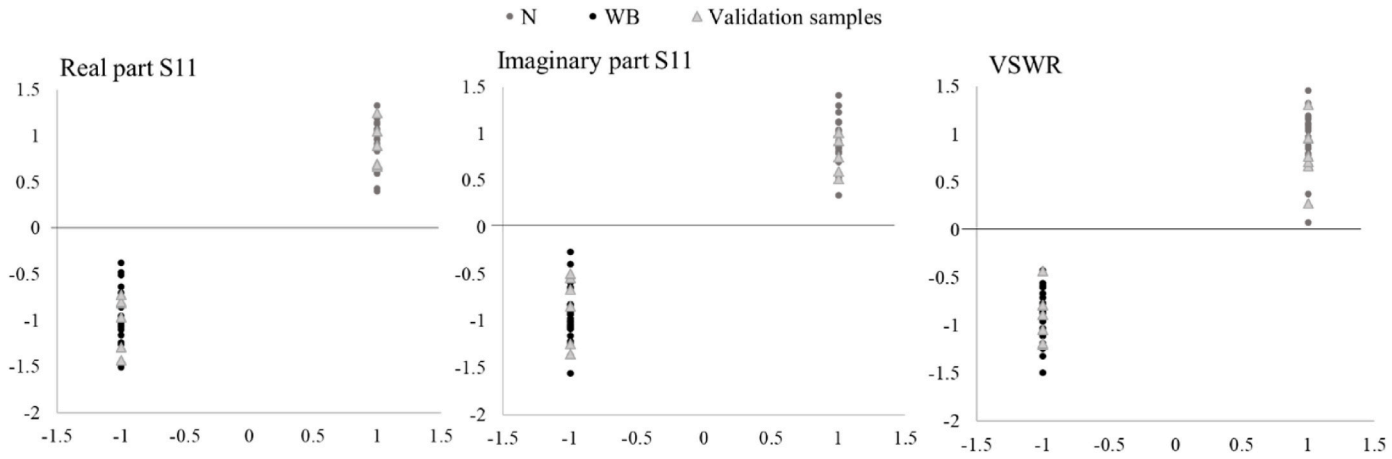

Fig. 9. Predicted versus measured values of the entire data set (calibration and validation) considering the real, imaginary part, and VSWR parameters of the PLS-DA classification; the two groups are unaffected (N) and affected (WB) breasts.

commit overestimation or underestimation, and by SEP the goodness of the models is confirmed.

RPD values between 2 and 3 indicate a fair model, between 3 and 4 good, and values greater than 4 excellent. Thus, the ability of PLS-DA to classify N and WB is primarily verified for the S11 real part that showed the best performance.

4. Conclusions

The dielectric constant and loss factor of chicken *Pectoralis major*

Table 1
Number of elements of the external validation data set, S11 real part, S11 imaginary part, VSWR, coefficient of determination (R^2) of calibration and validation and related root mean square error of prediction (RMSEP), standard error of prediction (SEP), systematic error BIAS, and the residual prediction deviation (RPD).

Validation coefficient	S11 Real part	S11 Imaginary part	VSWR
Elements	12	12	12
R^2 calibration	0.968	0.950	0.947
R^2 validation	0.935	0.896	0.889
RMSEP	0.26	0.32	0.33
SEP	0.26	0.33	0.34
Bias	−0.06	−0.03	−0.07
RPD	3.7	2.9	2.8

muscles exhibiting macroscopically normal appearance and affected by WB abnormality at 5°C showed changes as a function of the presence of the abovementioned quality defect. Accordingly, variations in dielectric data allowed the development of non-destructive, contactless, and rapid spectroscopic techniques, which are applicable in the processing line. An inexpensive instrumental chain based on a cavity antenna and a network vector analyzer was set up at the Interdepartmental Centre for Agri-Food Industrial Research located (Cesena, Italy) and it was exploited to automatically detect the chicken breast abnormality. The instrumentation proposed was tested and the results are very promising, correctly discriminating N and WB (100% of the external validation samples, n = 12). Further improvements of the research should focus on expanding the data set to increase the robustness of the statistical model. The diffusion on the market of extremely low-cost vector analyzers could further encourage the application of this technique.

CRediT authorship contribution statement

Eleonora Iaccheri: Writing – original draft, Methodology, Formal analysis, Data curation, Conceptualization. **Francesca Soglia:** Writing – original draft, Methodology, Formal analysis, Data curation, Conceptualization. **Massimiliano Petracci:** Writing – review & editing, Supervision. **Luigi Ragni:** Writing – review & editing, Supervision.

Declaration of competing interest

The authors declare that they have no known competing financial interests or personal relationships that could have appeared to influence the work reported in this paper.

Data availability

Data will be made available on request.

References

Asami, K., 2002. Characterization of Biological Cells by Dielectric Spectroscopy.

Barbut, S., Mitchell, R., Hall, P., Bacon, C., Bailey, R., Owens, C.M., Petracci, M., 2024. Myopathies in broilers: supply chain approach to provide solutions to challenges related to raising fast growing birds. *Poult. Sci.* 103, 103801. https://doi.org/10.1016/j.psj.2024.103801.

Caldas-Cueva, J.P., Mauromoustakos, A., Sun, X., Owens, C.M., 2021. Detection of woody breast condition in commercial broiler carcasses using image analysis. Poult Sci 100. https://doi.org/10.1016/j.psj.2020.12.074.

Choi, J., Shakeri, M., Kim, W.K., Kong, B., Bowker, B., Zhuang, H., 2024. Water properties in intact wooden breast fillets during refrigerated storage. Poult Sci 103. https://doi.org/10.1016/j.psj.2024.103464.

Ekramirad, N., Yoon, S.C., Bowker, B.C., Zhuang, H., 2024. Nondestructive assessment of woody breast myopathy in chicken fillets using optical coherence tomography imaging with machine learning: a feasibility study. Food Bioproc Tech. https://doi.org/10.1007/s11947-024-03369-1.

Geronimo, B.C., Mastelini, S.M., Carvalho, R.H., Barbon Júnior, S., Barbin, D.F., Shimokomaki, M., Ida, E.I., 2019. Computer vision system and near-infrared spectroscopy for identification and classification of chicken with wooden breast, and physicochemical and technological characterization. Infrared Phys. Technol. 96, 303–310. https://doi.org/10.1016/j.infrared.2018.11.036.

Iaccheri, E., Cevoli, C., Ragni, L., Rosa, M.D., Fabbri, A., 2023a. Physical stability of frozen eggplant: emphasis on state diagram, sorption, thermal, mechanical, and dielectric properties. Food Bioproc Tech 16, 1582–1594. https://doi.org/10.1007/s11947-023-03017-0.

Iaccheri, E., Laghi, L., Cevoli, C., Berardinelli, A., Ragni, L., Romani, S., Rocculi, P., 2015. Different analytical approaches for the study of water features in green and roasted coffee beans. J. Food Eng. 146, 28–35. https://doi.org/10.1016/j.jfoodeng.2014.08.016.

Iaccheri, E., Siracusa, V., Ragni, L., De Aguiar Saldanha Pinheiro, A.C., Romani, S., Rocculi, P., Dalla Rosa, M., Sobral, P.J. do A., 2023b. Studying physical state of films based on casava starch and/or chitosan by dielectric and thermal properties and effects of pitanga leaf hydroethanolic extract. J. Food Eng. 339. https://doi.org/10.1016/j.jfoodeng.2022.111280.

Kent, M., Anderson, D., 1996. Dielectric Studies of Added Water in Poultry Meat and Scallops.

Liu, S., Fukuoka, M., Sakai, N., 2012. Dielectric properties of fish flesh at microwave frequency. Food Sci. Technol. Res. 18, 157–166. https://doi.org/10.3136/fstr.18.157.

McKeown, M.S., Trabelsi, S., Tollner, E.W., Nelson, S.O., 2012. Dielectric spectroscopy measurements for moisture prediction in Vidalia onions. J. Food Eng. 111, 505–510. https://doi.org/10.1016/j.jfoodeng.2012.02.034.

Morey, A., Smith, A.E., Garner, L.J., Cox, M.K., 2020. Application of bioelectrical impedance analysis to detect broiler breast filets affected with woody breast myopathy. Front. Physiol. 11. https://doi.org/10.3389/fphys.2020.00808.

Mudalal, S., Lorenzi, M., Soglia, F., Cavani, C., Petracci, M., 2015. Implications of white striping and wooden breast abnormalities on quality traits of raw and marinated chicken meat. Animal 9, 728–734. https://doi.org/10.1017/S175173111400295X.

Nelson, S.O., 2010. Fundamentals of Dielectric Properties Measurements and Agricultural Applications. https://doi.org/10.1080/08327823.2010.11689778SSSS.

Nelson, S.O., Trabelsi, S., Zhuang, H., 2007. Dielectric Spectroscopy of Fresh Chicken Breast Meat.

Nunes, A.C., Bohigas, X., Tejada, J., 2006. Dielectric study of milk for frequencies between 1 and 20 GHz. J. Food Eng. 76, 250–255. https://doi.org/10.1016/j.jfoodeng.2005.04.049.

Pang, B., Bowker, B., Gamble, G., Zhang, J., Yang, Y., Yu, X., Sun, J.X., Zhuang, H., 2020a. Muscle water properties in raw intact broiler breast fillets with the woody breast condition. Poult Sci 99, 4626–4633. https://doi.org/10.1016/j.psj.2020.05.031.

Pang, Bin, Bowker, B., Zhang, J., Yang, Y., Zhuang, H., 2020b. Prediction of water holding capacity in intact broiler breast fillets affected by the woody breast condition using time-domain NMR. Food Control 118. https://doi.org/10.1016/j.foodcont.2020.107391.

Petracci, M., Soglia, F., Madruga, M., Carvalho, L., Ida, E., Estévez, M., 2019. Wooden-breast, white striping, and spaghetti meat: causes, consequences and consumer perception of emerging broiler meat abnormalities. Compr. Rev. Food Sci. Food Saf. https://doi.org/10.1111/1541-4337.12431.

Ragni, L., Al-Shami, A., Mikhaylenko, G., Tang, J., 2007. Dielectric characterization of hen eggs during storage. J. Food Eng. 82, 450–459. https://doi.org/10.1016/j.jfoodeng.2007.02.063.

Soglia, F., Laghi, L., Canonico, L., Cavani, C., Petracci, M., 2016. Functional property issues in broiler breast meat related to emerging muscle abnormalities. Food Res. Int. 89, 1071–1076. https://doi.org/10.1016/j.foodres.2016.04.042.

Soglia, F., Petracci, M., Davoli, R., Zappaterra, M., 2021. A critical review of the mechanisms involved in the occurrence of growth-related abnormalities affecting broiler chicken breast muscles. Poult Sci. 100, 101180. https://doi.org/10.1016/j.psj.2021.101180.

Sun, X., You, J., Maynard, C.J., Caldas-Cueva, J.P., Giampietro-Ganeco, A., Owens, C.M., 2022. Assessment of meat quality distributions of breast fillets with woody breast condition in the raw and cooked state. J. Food Sci. Technol. 59, 3557–3566. https://doi.org/10.1007/s13197-022-05353-z.

Tanaka, F., Mallikarjunan, P., Kim, C., Hung, Y.-C., 2000. Measurement of dielectric properties of chicken breast meat. Journal of the Japanese Society of Agricultural Machinery 62 (4), 109–119. https://doi.org/10.11357/jsam1937.62.4_10.

Tasoniero, G., Bertram, H.C., Young, J.F., Dalle Zotte, A., Puolanne, E., 2017. Relationship between hardness and myowater properties in Wooden Breast affected chicken meat: a nuclear magnetic resonance study. LWT 86, 20–24. https://doi.org/10.1016/j.lwt.2017.07.032.

Trabelsi, S., 2015. Variation of the dielectric properties of chicken meat with frequency and temperature. J. Food Meas. Char. 9, 299–304. https://doi.org/10.1007/s11694-015-9235-6.

Traffano-Schiffo, M.V., Castro-Giraldez, M., Colom, R.J., Talens, P., Fito, P.J., 2021. New methodology to analyze the dielectric properties in radiofrequency and microwave ranges in chicken meat during postmortem time. J. Food Eng. 292. https://doi.org/10.1016/j.jfoodeng.2020.110350.

Tran, V.N., Stuchly, S.S., 1987. Dielectric properties of beef, beef liver, chicken and salmon at frequencies from 100 to 2500 MHz. J. Microw. Power Electromagn. Energy 22, 29–33. https://doi.org/10.1080/08327823.1987.11688003.

Wang, C., Che, S., Susta, L., Barbut, S., 2023. Textural and physical properties of breast fillets with myopathies (wooden breast, white striping, spaghetti meat) in Canadian fast-growing broiler chickens. Poult. Sci. 102, 102309. https://doi.org/10.1016/j.psj.2022.102309.

Wold, J.P., Veiseth-Kent, E., Høst, V., Løvland, A., 2017. Rapid on-line detection and grading of wooden breast myopathy in chicken fillets by near-infrared spectroscopy. PLoS One 12. https://doi.org/10.1371/journal.pone.0173384.

Wold, S., Sjöström, M., Eriksson, L., 2001. PLS-regression: a basic tool of chemometrics. Chemometr. Intell. Lab. Syst. 58, 109–130. https://doi.org/10.1016/S0169-7439(01)00155-1.

Yoon, S.C., Bowker, B.C., Zhuang, H., Lawrence, K.C., 2022. Development of imaging system for online detection of chicken meat with wooden breast condition. Sensors 22. https://doi.org/10.3390/s22031036.

Zhang, J., Bowker, B., Yang, Y., Pang, B., Yu, X., Tasoniero, G., Zhuang, H., 2022. Water properties and marinade uptake in broiler pectoralis major with the woody breast condition. Food Chem. 391. https://doi.org/10.1016/j.foodchem.2022.133230.

Zhang, Y., Wang, P., Xu, X., Xia, T., Li, Z., Zhao, T., 2020. Effect of wooden breast myopathy on water-holding capacity and rheological and gelling properties of chicken broiler breast batters. Poult Sci 99, 3742–3751. https://doi.org/10.1016/j.psj.2020.03.032.